PLASMA SHAPE AND FUELING DEPENDENCE ON THE SMALL ELMS REGIME IN TCV AND AUG

B. LABIT, H. DE OLIVERA, R. MAURIZIO, A. MERLE, P. MOLINA, U. SHEIKH
École Polytechnique Fédérale de Lausanne (EPFL), Swiss Plasma Center (SPC)
Lausanne, Switzerland
Email: benoit.labit@epfl.ch

T. EICH, M. BERNERT, M. DUNNE, J. STOBER, E. WOLFRUM
Max-Planck-Institut für Plasmaphysik
Garching, Germany

G. F. HARRER
Fusion@OEAW, TU Wien,
TU Wien
Vienna, Austria

L. FRASSINETTI
Division of Fusion Plasma Physics, KTH Royal Institute of Technology
Stockholm, Sweden

P. HENNEQUIN
LPP, CNRS, Ecole Polytechnique
Palaiseau, France

H. MEYER, S. SAARELMA
CCFE, Culham Science Centre
Abingdon, United Kingdom

TCV TEAM*

AUG TEAM†

EUROfusion MST1 TEAM‡

Abstract

A series of experiments has been conducted at AUG and TCV to disentangle the role of fueling, plasma triangularity and closeness to a double null (DN) configuration for the onset of the small ELM regime. At AUG, the role of the SOL density has been revisited. Indeed, it turns out that a large density SOL is not a sufficient condition to achieve the Type-II (small) ELM regime. This has been demonstrated with a constant gas fueled plasma close to DN which has been progressively shifted down, relaxing therefore the closeness to DN at constant δ (q_{95}=4.5, κ=1.8, f_G=0.85, δ=0.4). As the plasma is moved down, Type-I ELMs are progressively restored, finally being the unique ELM regime. Since the entire pedestal profiles are unchanged by the transition from Type-II to Type-I ELMs, we conclude that the separatrix density is not the unique key parameter. At TCV, a systematic scan in the fueling rate has been done for a medium triangularity plasma shape (q_{95}=4.5, κ=1.5, f_G=0.4-0.5, δ=0.4). As the D2 fueling is increased, the Type-I ELM frequency decreases and small ELMs are observed in between large ones. The mixed ELM regime is accompanied by an increase of the density at the separatrix. Increasing the triangularity from δ=0.38 to δ=0.54 (q_{95}=4.5, κ=1.5, f_G=0.45) is sufficient to have a well-controlled density with fully stabilized Type-I ELMs and only grassy ELMs. In this regime, the global confinement is maintained and the peak heat flux at the outer target is reduced by a factor of 10. The pedestal stability analysis shows that the intermediate-*n* peeling-ballooning boundary expands considerably in the high triangularity case, suggesting that grassy ELMs are caused by high-*n* ballooning modes affecting a much smaller region of the pedestal.

---

* See the author list of "S. Coda et al 2017, Nucl. Fusion. 57 102011"

† See the author list of "A. Kallenbach et al 2017, Nucl. Fusion. 57 102015"

‡ See the author list of "H. Meyer et al 2017 Nucl. Fusion 57 102014"

1. INTRODUCTION

To achieve its goals, ITER has to operate in the H-mode confinement regime. Nevertheless, this regime with good confinement is usually accompanied with Type-I ELMs, which may lead to a too strong erosion of the divertor strike point region. An attractive solution to overcome this limitation is to operate in the Type-II ELM regime [1-4], for which the good confinement is maintained w.r.t. to Type-I but the target heat loads are strongly reduced. Usually, the key ingredients to achieve this regime are to operate at high plasma triangularity, actually close to a double-null (DN) configuration and at high density ($n_{e,av}/n_G>0.85$). In addition, the onset of Type-II ELMs is observed to be related to plasma conditions around the separatrix since, for similar pedestal profiles, a gas fueled discharge shows Type-II ELMs while a pellet fueled discharge features also Type-I ELMs, the separatrix density being reduced in the latter case [5,6]. Recently, a series of experiments has been conducted at AUG and TCV, under the umbrella of the EUROFusion work package on Medium Sized Tokamaks, to disentangle the role of fueling, plasma triangularity and closeness to the DN configuration for the onset of the small ELM regime.

2. MIXED ELM REGIME AT TCV AT LARGE SEPARATRIX DENSITY

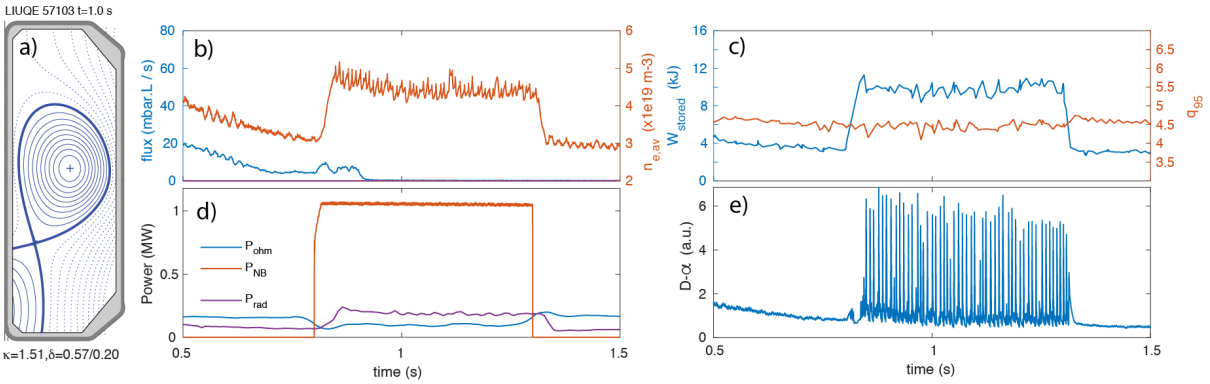

Figure 1 : Summary of TCV shot 57103 – a reference Type-I ELMy H-mode a) plasma shape; b) D2 fueling level and line average density; c) stored energy and q_{95}; d) Added and radiated powers; e) D-α signal

A reliable scenario for Type-I ELMy H-mode at TCV is obtained with the following parameters: LSN, I_p = 140 kA, B_T = 1.4 T, κ = 1.5, δ=0.38, q_{95}=4.5, P_{NBI} = 1 MW (P_{L-H} ~0.7MW at $n_{el}=3x10^{19}m^{-3}$) and it is summarized in Fig.1. This scenario has been used to investigate the effect of impurity seeding on the pedestal properties [7, 8]. Even though the gas fueling is negligible, the plasma density is maintained constant by a sufficient wall recycling from the graphite tiles. The ELMs are monitored with a photodiode measuring the D-α radiation along a vertical line-of-sight. The pedestal profiles are obtained from a recently upgraded Thomson scattering system [9] and fitted with a modified hyperbolic tangent function. Moreover, the profiles have to be shifted such that $T_{e,sep}$ = 50 eV (as inferred from the 2-point model) when one wants to compute the peeling-ballooning stability of the pedestal.

A key ingredient to achieve the Type-II ELM regime is to operate at large density at the separatrix ($f_{GW,ped} \geq 0.8$) which can be controlled with gas fueling. A mix of Type-I and small ELMs regime has been realized at TCV. Indeed, starting from the reference Type-I ELM regime, a scan in deuterium fueling has been performed on a shot to shot basis (Fig. 2). As the D2 flow increases, the following observations can be made: 1) the Type-I ELM frequency decreases up to a factor of 2 while the relative loss energy ΔW/W remains around 11% (Fig. 3a); 2) the baseline level of the D-α signal increases which might indicate an elevation of the recycling level and 3) small ELMs, in between Type-I, are becoming more and more frequent. The typical frequency of these small ELMs is about 2.5 kHz. A consequence of the reduced Type-I ELM frequency is that the plasma density is not anymore controlled and it increases with time, eventually leading to a back transition into L-mode. The lost energy associated with the small ELMs is below 1% which corresponds to the diagnostic resolution.

The stored energy is not notably affected (Fig 3b) since the pedestal temperature is reduced by 15% at the end of the fueling scan while the pedestal density increases by the same amount (Fig. 3c). The density growth at the pedestal is less rapid than the separatrix density elevation, the latter being evaluated once the profiles have been shifted to satisfy $T_{e,sep}$=50 eV. As a consequence the ratio $n_{e,sep}$ / $n_{e,ped}$ increases by a factor 2 from 0.25 to 0.5 (Fig. 3c). Despite the fact that the wall recycling is increasing, no significant carbon accumulation in the plasma core

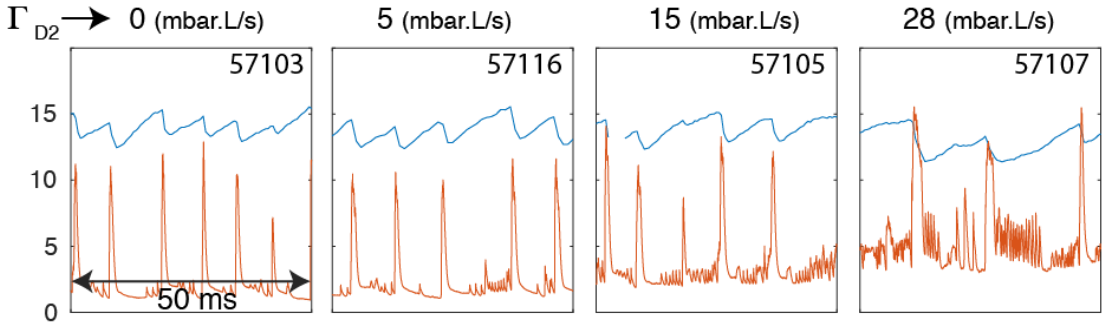

Figure 2 : Fueling scan for TCV medium triangularity plasmas: D-α signal (red) and stored energy in kJ (blue).

is observed leading to a reduced fraction of core radiation with gas fueling (Fig. 3d).

In addition, even though an outward shift of the density pedestal is observed [7,8] with increasing fueling (Fig. 3e), leading to a reduction of the peeling-ballooning stability, no evidence of a high density front at the high field side [10] is reported so far from TCV, conversely to AUG. This might be due to the TCV open divertor geometry and will be reassessed once the divertor will be closed with baffles [11]. Target heat loads during ELMs have been estimated from infrared measurements [12]. The target peak heat flux associated with Type-I ELM remains fairly constant through the fueling scan consistent with ΔW/W being almost unaffected.

Finally, since no broadband turbulence has been observed on the magnetic probes, it cannot be concluded if these small ELMs are Type-II. Nevertheless, a similar fueling scan for plasmas at higher triangularity, discussed in Ref. [7], also shows a transition to a mix ELM regime, with in this case a signature of turbulence in the frequency range [20-40] kHz on the magnetics.

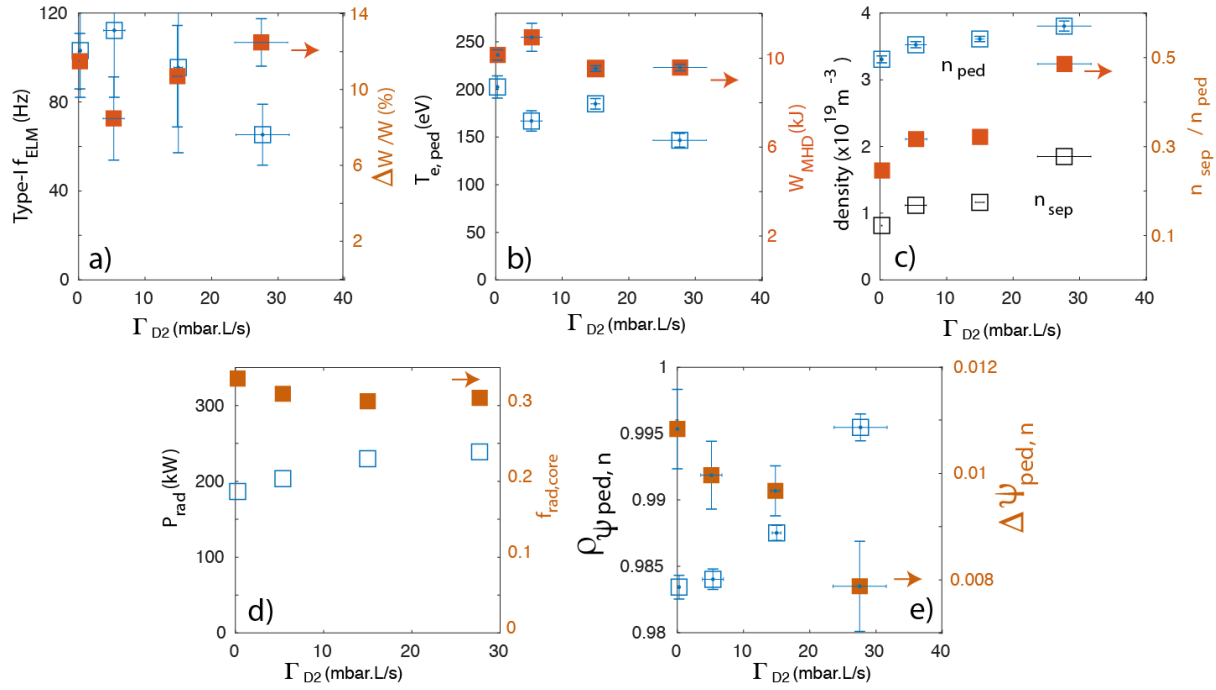

Figure 3 : a) Type-I ELM frequency and relative loss energy; b) Pedestal temperature and stored energy; c) Density at the pedestal top, at the separatrix and ratio of both; d) Radiated power and core radiated fraction; e) Density pedestal position and pedestal width. All quantities are plotted against the D2 flow.

3. GRASSY ELM REGIME AT TCV FOR PLASMAS WITH HIGH TRIANGULARITY

Type-II and/or grassy ELMs are usually observed at large plasma triangularity [2,13]. A grassy ELM regime has also been achieved at TCV. Two discharges (LSN, I_p=140 kA, B_T=1.4 T) have been performed with the exact same parameters except the upper triangularity which changes from δ_u=0.1 (#61057) to δ_u=0.32 (#61056) as shown in Fig. 4 a). For the high triangularity case, the configuration is close to DN (with a distance, at the outboard

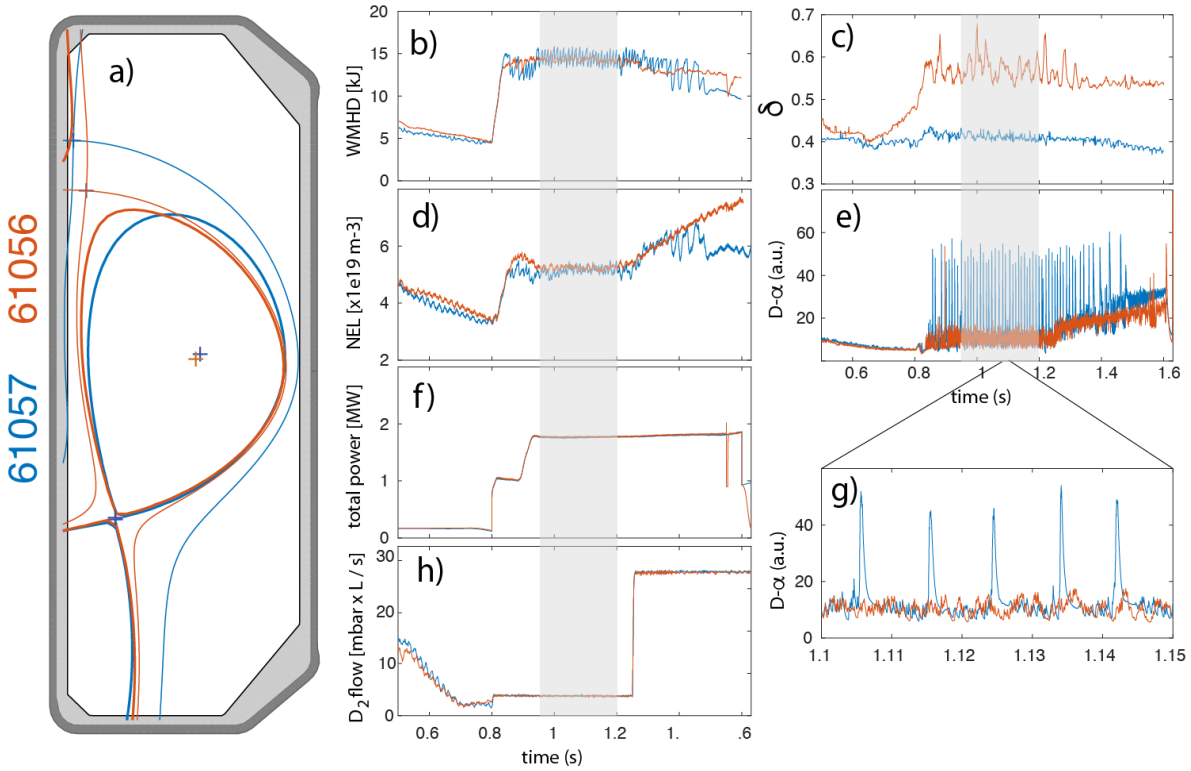

Figure 4: Time evolution of main plasma parameters for TCV shots 61056 and 61057, differing only by the upper triangularity. At large triangularity (and also close to DN), the type-I ELMs are fully suppressed.

midplane, between the separatrix and the flux surface through the secondary X-pt Δ_{sep}=6 mm~$2\lambda_q$, with λ_q~0.69 $B_{p,u}^{-1.19}$ [14]). Both plasmas are heated with 1MW of NBI plus 0.75 MW of X3 ECRH (Fig. 4f). The same constant D2 flow (3.8 mbar.L/s) has been imposed at the L-H transition giving $n_{e,sep}/n_{e,ped}$~0.25. For the medium triangularity discharge, the ELMs are large Type-I ELMs (f_{ELM} = 100 Hz, $\Delta W/W$~10%) while for the high triangularity discharge, Type-I ELMs are fully suppressed and replaced by grassy high frequency ELMs for which $\Delta W/W$<1%. Later in the discharge, the fuelling was increased by a factor of 8, resulting for the high triangularity case, to an increase of the plasma density up to an H-mode density limit disruption. For the medium triangularity shape, the Type-I ELMs frequency decreases so the density increases and a back-transition to L-mode is observed (Fig 4 d). Although, at low fueling rate, the plasma confinement usually improves when the triangularity is increased [15], here, the stored energy is the same for both triangularities. In Fig. 5 a-b), the temperature and density pedestal profiles are plotted. They are remarkably similar for both discharges even though the kinetic profiles are selected in the [75%-90%] phase of the Type-I ELM cycle while they are time averaged for the grassy ELM case. As a consequence, the pedestal pressure is only increased by less than 5% for the large δ case. Some plasma and pedestal parameters are compared in Table 1. For both plasmas, the target heat loads have been estimated at the outer strike point. Compared to the Type-I regime, the peak heat flux is reduced by a factor of about 10 with the grassy ELM regime, reaching similar levels than the inter-Type-I ELMs (Fig. 5 c).

ELM regime	q_{95}	δ	Type-I f_{ELM} (Hz)	$\Delta W/W$	$T_{e,ped}$ (eV)	$n_{e,ped}$ ($x10^{19}$ m^{-3})	$n_{e,sep}$ ($x10^{19}$ m^{-3})	$\nu^*_{,ped}$	β_{pol}	$f_{GW,ped}$	W_{MHD} (kJ)	H_{98y2}
Type-I	4.7	0.38	100	9%	227	3.8	0.9	2.66	1.13	0.34	13	1.45
grassy	4.7	0.54	-	<1%	255	3.5	0.8	1.95	1.13	0.32	13	1.3

Table 1: Plasma and pedestal parameters comparing the Type-I and small/grassy ELM regimes at TCV. They have been averaged over the time window indicated by the shaded area in Fig. 4.

In line with JT60-U results [16], when the input power is reduced (1 MW NBI only) the Type-I ELMs are not fully suppressed for large δ and a regime of mixed ELMs is established as for the medium triangularity scenario discussed in the previous section.

For both plasmas, the pedestal stability has been studied using the ELITE code to obtain the $j-\alpha$ stability diagram and the self-consistent path in the $j-\alpha$ space [17]. Here, j is the current density and α is the normalized pedestal pressure gradient. The equilibrium has been calculated using the HELENA code [18], using as input the

fits to the experimental T_e and n_e profiles. The stability diagram is shown in Fig. 5 d). The pedestal pressure gradient rise by about 10% for the high-δ case together with the 10% increase of the safety factor close to separatrix, lead to a 20% growth for the α_{max} value. While the $n=\infty$ ballooning boundary (unstable region at the bottom of the pedestal) is affected only a little by the change of the plasma shape, the intermediate-n peeling-ballooning boundary expands considerably in the high triangularity case. This could indicate that while the large Type-I ELMs are caused by the peeling-ballooning modes covering the entire pedestal, these modes are not accessible for high triangularity pedestals. The grassy ELMs are then caused by high-n ballooning modes affecting a much smaller region of the pedestal.

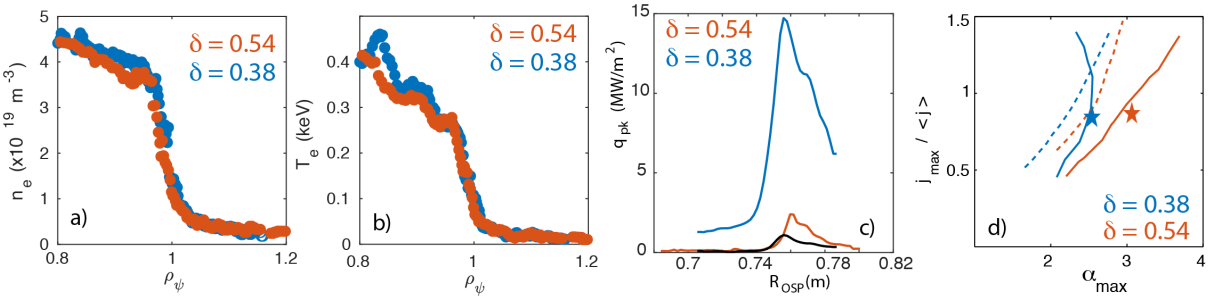

Figure 5. For δ=0.38 (blue) and δ=0.54 (orange): a) Pedestal density profile; b) Pedestal temperature profile; c) Outer strike point peak heat flux profile; The black curve is the inter-Type-I profile. d) Stability diagram with the finite-n stability boundary (solid) and the n=∞ ballooning mode boundary (dashed).

4. EFFECT OF CLOSENESS TO DOUBLE-NULL ON THE TYPE-II ELMY REGIME AT AUG

At AUG, Type-I ELMs are partially restored from a pure Type-II ELM when the gas fuelling from the SOL is replaced by pellet injection into the plasma core [5], resulting in a reduced density at the separatrix (Fig 6 b; black). However, the role of the SOL density has been recently revisited [6]. Indeed, it turns out that a large separatrix density ($n_{e,sep}$~3x10^{19}m^{-3}), which is correlated with the ballooning parameter α_{sep} [19], is not a sufficient condition to achieve the Type-II regime. This has been demonstrated with a constant gas fueled plasma (q_{95}=4.5, κ=1.6, δ=0.37), close to DN (Δ_{sep}=7-9 mm), which has been progressively shifted down, relaxing therefore the closeness to DN (Δ_{sep}=14 mm) at almost constant δ. As the plasma is moved down, Type-I ELMs are progressively restored, leading to a mix of ELM types (Fig. 6 a). It is observed that the pedestal profiles (Fig. 6 b-c) are almost

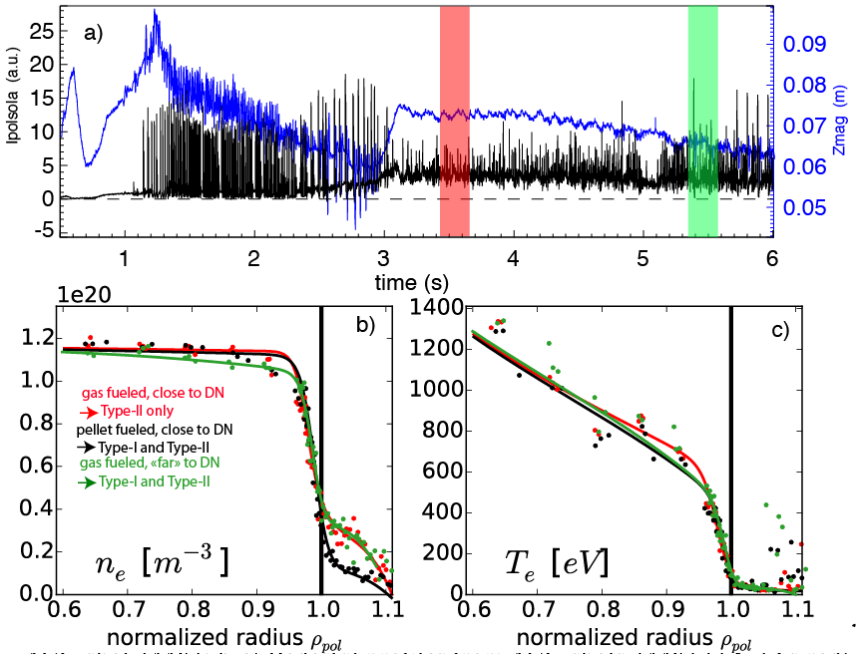

AUG shot 34483; b-c) Pedestal profiles from AUG shots 34483 (5.5-5.6s red), 34462 (5.5-5.6 s, black) and 34483 (5.2-5.3 s, green).

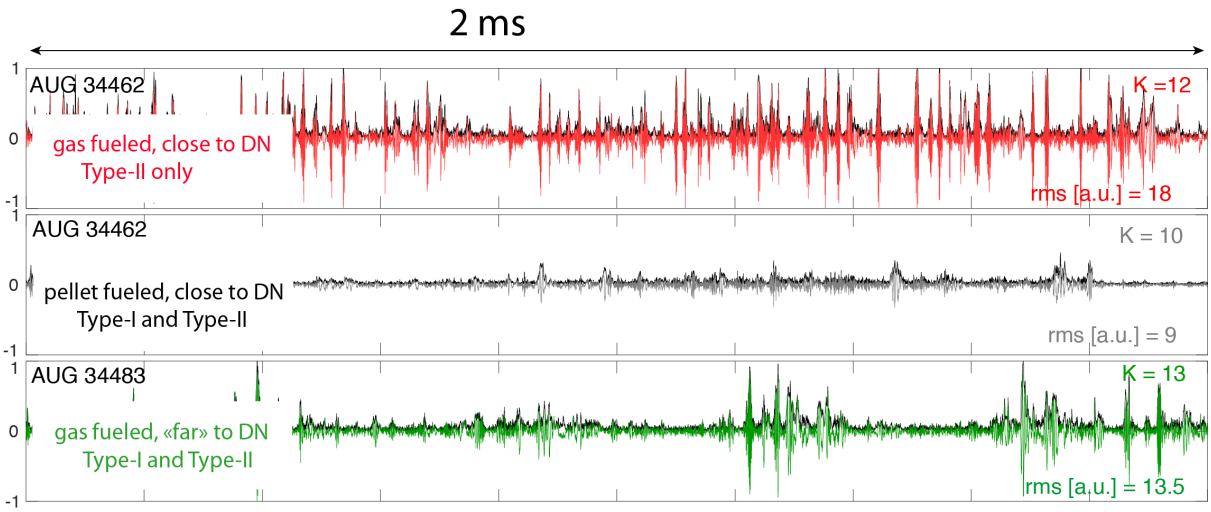

Figure 7 : Reflectometry amplitude signals (2ms long) measured at ρ_ψ~0.99 for the three phases discussed in Figure 6;

unchanged for both phases. Not only the pedestal top profiles are unchanged, but also the SOL profiles remained unaffected by the transition from pure Type-II to a mix of Type-II and Type-I ELMs.

A common feature of Type-II ELMs is a broadband turbulence around 30 kHz usually observed on the ECE or magnetic signals [3]. In addition, the filamentary transport at the foot of the pedestal is found to significantly change from Type-I to Type-II as observed on MAST [20]. This is confirmed from Doppler Back Scattering measurements just inside the separatrix (ρ~0.99). Figure 7 shows 2 ms long time series of DBS amplitude signals measured in the three phases. For the pure Type-II ELM regime (DN and gas fueling, red), DBS signal shows large bursts in amplitude. These bursts, in the range 40-80 kHz, are much more frequent than for the mixed ELM regime (close to DN and pellet fueling, black) [21]. Nevertheless, the mixed ELM regime far from DN with gas fueling (green curve) is also characterized by strong intermittency in the DBS signal. This requires further investigations but it suggests a correlation with the filamentary transport in the scrape-off layer close to the H-mode density limit [22]. The strong dependence of the small ELMs on the separatrix density suggests they are modes localized near the separatrix. It turns out that once the closeness to DN is relaxed, the poloidal averaged magnetic shear in the immediate vicinity of the separatrix is slightly larger than for the configuration close to DN. Therefore, it is conjectured that the small ELMs are stabilized by this increased shear and only Type-I ELMs remain unstable [6].

5. DISCUSSION AND OUTLOOK

	q_{95}	δ	β_{pol}	ν^*_{ped}	$f_{GW,ped}$	$n_{e,sep}/n_{e,ped}$
AUG (type-II)	4.5	0.37	1.2	1.39	0.82	0.4
TCV (grassy)	4.5	0.54	1.3	1.95	0.32	0.2
ITER	3	0.4	0.6	0.1	0.6-0.8	-

Table 2 : Adimensional parameters for which type-II ELMs in AUG and grassy ELMs at TCV are achieved. For comparison, the ITER operational parameters are also given.

The experimental results from AUG and TCV discussed here are in line with our current understanding about the physical mechanism [6] which drives small/Type-II ELMs. It can be summarized as follows: at short Δ_{sep} and/or high δ, ballooning modes become unstable in a region just inside the separatrix. They modify the pressure profile by flattening the region around the separatrix, such that the remaining pedestal width, which determines the stability of the peeling-ballooning modes, becomes narrower. This has a stabilizing influence on type-I ELMs. These local ballooning modes are driven by the pressure gradient just inside the separatrix, therefore a high separatrix density drives them unstable. At the same time, they are stabilized by an increased shear, which has been identified to be affected by the closeness to DN in the AUG experiment. High triangularity is necessary,

because only high δ allows to achieve such high separatrix pressures without the type-I ELMs appearing first, because the high δ stabilizes peeling-ballooning ELMs.

To conclude, the key ingredients required to achieve a small ELM regime with good confinement and reduced target heat loads summarized in Table 2. A large density at the separatrix ($n_{e,sep}/n_{e,ped}\geq0.4$) is needed at medium triangularity (δ~0.4). This condition can be loosened ($n_{e,sep}/n_{e,ped}\sim0.2$) at a larger averaged triangularity (δ~0.5). Nevertheless, it is difficult to disentangle between a pure effect of a large top triangularity and the effect of being close to a DN configuration. Indeed, it has to be noted that in the AUG scenario, the maximum fueling rate is already established at t=2.2s and it is only once the plasma has been shifted up (t=3.0-3.1 s) that the separatrix density increases and the pure type-II ELMs are obtained. However, the magnetic configuration has become closer to DN at the same time the top triangularity is increased. The difficulty to separate δ and Δ_{sep} is even more obvious for the TCV experiments (Fig. 5 a): δ=0.38 (0.54) corresponds to Δ_{sep} = 28 mm (6 mm), respectively. From the grassy ELM regime, a possible future experiment for TCV could be to reduce the bottom triangularity to achieve an average δ~0.4, keeping Δ_{sep} unchanged and see if the Type-I ELMs are recovered. If it will be confirmed that a short Δ_{sep} ($<5\lambda_q$) is a stringent condition to achieve small ELM regimes, an extrapolation to ITER might be difficult since $\Delta_{sep,\,ITER}\sim4$ cm >> $\lambda_{q,\,ITER}$.

Another possible difficulty to extrapolate an existing small ELM regime to ITER is the necessity to match simultaneously the pedestal density ($f_{GW,ped}>0.6$) and the low collisionality ν^*_{ped}. In present devices, both parameters are strongly coupled through their dependence on the plasma current and it is not easy to break this coupling at $q_{95}>4$. Future experiments might need to achieve small ELM regime at larger I_p, including $q_{95}<3$, to investigate the possibility to decouple $f_{GW,ped}$ and ν^*_{ped}.

Definitely, Type-I and small/Type-II ELMs can exist at the same time, suggesting they are excited by different physical mechanisms. However, the underlying instabilities leading to small/Type-II ELMs have not yet been revealed and further experiments devoted to a better understanding of the pedestal and SOL turbulence and particle and heat transport are required. This will be complemented by further development of theoretical models for small/no ELM regimes and by nonlinear MHD simulations using global codes in order to gain for confidence in terms of their compatibility to ITER plasmas.

ACKNOWLEDGEMENTS

This work has been carried out within the framework of the EUROfusion Consortium and received funding from the Euratom research and training programme 2014-2018 under Grant Agreeement No. 633053. The views and opinions expressed herein do not necessarily reflect those of the European Commission. G. F. Harrer is a fellow of the Friedrich Schiedel Foundation for Energy Technology.

REFERENCES

[1] STOBER J. et al, Type II ELMy H modes on ASDEX Upgrade with good confinement at high density, Nucl. Fusion **41** (2001) 1123

[2] OYAMA N. et al, Pedestal conditions for small ELM regimes in tokamaks, Plasma Phys. Control. Fusion **48** (2006) A171

[3] WOLFRUM E. et al, Characterization of edge profiles and fluctuations in discharges with Type-II and nitrogen-mitigated edge localized modes in ASDEX Upgrade, Plasma Phys. Control. Fusion **53** (2011) 085026

[4] VIEZZER E., et al, Access and sustainment of naturally ELM-free and small-ELM regimes, Nucl. Fusion **58** (2018) 115002

[5] MEYER H. et al, Overview of progress in European medium sized tokamaks towards an integrated plasma-edge/wall solution, Nucl. Fusion **57** (2017) 201014

[6] HARRER G. F. et al., Parameter dependences of small edge localized modes (ELMs), Nucl. Fusion **58** (2018) 112001

[7] SHEIKH U. et al, Pedestal Structure and Energy Confinement Studies on TCV, submitted to Plasma Physics and Controlled Fusion (2018)

[8] FRASSINETTI L., et al, “Role of the pedestal position on the pedestal performance in AUG, JET-ILW and TCV and implications for ITER”, this conference, EX/P8-22
[9] HAWKE J. et al., Improving spatial and spectral resolution of TCV Thomson scattering, Journal of Instrumentation, **12** (2017) C12005
[10] DUNNE, M.G., et al, The role of the density profile in the ASDEX-Upgrade pedestal structure, Plasma Phys. Control. Fusion **59** (2017) 014017
[11] REIMERDES H. et al, TCV divertor upgrade for alternative magnetic configurations, Nuclear Material and Energy, **12** (2017) 1106
[12] MAURIZIO R. et al, Divertor power load studies for attached L-mode single-null plasmas in TCV Nucl. Fusion **58** (2018) 016052
[13] EICH T. et al, Scaling of the tokamak near the scrape-off layer H-mode power width and implications for ITER, Nucl. Fusion **53** (2013) 093031
[14] KAMADA Y. et al, Disappearance of giant ELMs and appearance of minute grassy ELMs in JT-60U high-triangularity discharges, Plasma Phys. Control Fusion **42** (2000) A247
[15] STOBER J. et al, Effects of triangularity on confinement, density limit and profile stiffness of H-modes on ASDEX upgrade, Plasma Phys. Control. Fusion **42** (2000) A211
[16] OYAMA N. et al, Energy loss for grassy ELMs and effects of plasma rotation on the ELM characteristics in JT-60U, Nucl. Fusion **45** (2005) 871
[17] SNYDER P.B. Pedestal stability comparison and ITER pedestal prediction, Nucl. Fusion **49** (2009) 085035
[18] SAARELMA S., *et al*. MHD stability analysis of small ELM regimes in JET Plasma Phys. Control. Fusion **51** (2009) 035001.
[19] EICH T. et al, Correlation of the tokamak H-mode density limit with ballooning stability at the separatrix, Nucl. Fusion **58** (2018) 034001
[20] KIRK A., et al, Comparison of the filament behaviour observed during Type I ELMs in ASDEX upgrade and MAST Journal of Physics: Conference Series **123**, (2008) 1
[21] HENNEQUIN P., et al, “Inter-ELM Fluctuations and Flows and their evolution when approaching the density limit in the ASDEX Upgrade tokamak”, 44th EPS Conference on Plasma Physics, Belfast, Northern Ireland, (2017).
[22] VIANELLO N. et al, “Scrape-off layer (SOL) transport and filamentary dynamics in high density tokamak regimes”, this conference, EX/P8-13